Restoration of Glucose-Stimulated Cdc42-Pak1 Activation and Insulin Secretion by a Selective Epac Activator in Type 2 Diabetic Human Islets

Rajakrishnan Veluthakal,[1] Oleg G. Chepurny,[2] Colin A. Leech,[2,3] Frank Schwede,[4] George G. Holz,[2,5] and Debbie C. Thurmond[1]

Diabetes 2018;67:1999–2011 | https://doi.org/10.2337/db17-1174

Glucose metabolism stimulates cell division control protein 42 homolog (Cdc42)-p21-activated kinase (Pak1) activity and initiates filamentous actin (F-actin) cytoskeleton remodeling in pancreatic β-cells so that cytoplasmic secretory granules can translocate to the plasma membrane where insulin exocytosis occurs. Since glucose metabolism also generates cAMP in β-cells, the cross talk of cAMP signaling with Cdc42-Pak1 activation might be of fundamental importance to glucose-stimulated insulin secretion (GSIS). Previously, the type-2 isoform of cAMP-regulated guanine nucleotide exchange factor 2 (Epac2) was established to mediate a potentiation of GSIS by cAMP-elevating agents. Here we report that nondiabetic human islets and INS-1 832/13 β-cells treated with the selective Epac activator 8-pCPT-2′-*O*-Me-cAMP-AM exhibited Cdc42-Pak1 activation at 1 mmol/L glucose and that the magnitude of this effect was equivalent to that which was measured during stimulation with 20 mmol/L glucose in the absence of 8-pCPT-2′-*O*-Me-cAMP-AM. Conversely, the cAMP antagonist Rp-8-Br-cAMPS-pAB prevented glucose-stimulated Cdc42-Pak1 activation, thereby blocking GSIS while also increasing cellular F-actin content. Although islets from donors with type 2 diabetes had profound defects in glucose-stimulated Cdc42-Pak1 activation and insulin secretion, these defects were rescued by the Epac activator so that GSIS was restored. Collectively, these findings indicate an unexpected role for cAMP as a permissive or direct metabolic coupling factor in support of GSIS that is Epac2 and Cdc42-Pak1 regulated.

Type 2 diabetes (T2D) is associated with defects of glucose-stimulated insulin secretion (GSIS) in which pancreatic β-cells fail to compensate for peripheral insulin resistance so that hyperglycemia ensues (1). GSIS is complex and requires the concerted actions of multiple cellular processes, including plasma membrane glucose transport, conversion of glucose to glucose-6-phosphate, and glycolytic or mitochondrial metabolism that generates key ionic (Ca^{2+}) and metabolic coupling factors (ATP, glutamate, NADPH, monoacylglycerol) (2). In vitro studies of the human β-cell response to a stepwise increase of glucose concentration reveal that insulin secretion is biphasic (3,4). A first-phase of GSIS results from exocytosis of a readily releasable pool of secretory granules prepositioned at the plasma membrane (3,4). A subsequent second-phase of GSIS involves active translocation of a reserve pool of secretory granules from the cytoplasm to the plasma membrane (3,4). Secretory granule translocation requires actin cytoskeletal remodeling, and defects in this remodeling might explain, at least in part, the insulin secretory defect that is characteristic of T2D (5–7).

During the second phase of GSIS, there occurs sequential activation of cell division control protein 42 homolog (Cdc42; a Rho family GTPase) and its downstream effector, the p21-activated kinase (Pak1; a Ser/Thr protein kinase) (5–7). This pathway leads to the remodeling of a cortical filamentous actin (F-actin) network that exists immediately beneath the plasma membrane (8). During the fasting state when levels of blood glucose are low, cortical F-actin

[1]Department of Molecular and Cellular Endocrinology, Diabetes and Metabolism Research Institute, Beckman Research Institute of City of Hope, Duarte, CA
[2]Department of Medicine, State University of New York, Upstate Medical University, Syracuse, NY
[3]Department of Surgery, State University of New York, Upstate Medical University, Syracuse, NY
[4]BIOLOG Life Science Institute, Bremen, Germany
[5]Department of Pharmacology, State University of New York, Upstate Medical University, Syracuse, NY

Corresponding author: Rajakrishnan Veluthakal, rveluthakal@coh.org.

Received 29 September 2017 and accepted 29 June 2018.

This article contains Supplementary Data online at http://diabetes.diabetesjournals.org/lookup/suppl/doi:10.2337/db17-1174/-/DC1.

restricts the access of secretory granules to their release sites. However, in response to a postprandial increase of blood glucose, localized cortical F-actin remodeling enables secretory granules to translocate to the plasma membrane for second-phase GSIS (5–7). It is generally accepted that β-cell glucose metabolism is the primary stimulus for Cdc42-Pak1–induced F-actin remodeling and that a key biochemical event is the association of Cdc42 with Cool-1/βPix, a guanine nucleotide exchange factor (GEF) that converts inactive Cdc42-guanosine 5′-diphosphate (GDP) to active Cdc42-guanosine 5′-triphosphate (GTP) (9). Islets from individuals with T2D are 80% deficient in Pak1 protein expression when compared with islets of individuals without diabetes (6), yet it is still uncertain whether Pak1 activation by Cdc42 is altered in the context of T2D.

It is increasingly apparent that the second messenger cAMP participates in the process of GSIS and that insulin exocytosis is under the control of cAMP-dependent protein kinase (PKA; a Ser/Thr protein kinase) and also cAMP-regulated GEFs (Epacs) (10,11). The conventional view is that agonist binding to G-protein–coupled receptors (GPCRs) leads to cAMP production that is catalyzed by transmembrane adenylyl cyclases (tmACs). In fact, GSIS is strongly potentiated by the cAMP-elevating hormone glucagon-like peptide 1 (GLP-1) acting at its GPCR expressed on β-cells (10,11). However, there is additional evidence that glucose metabolism per se in β-cells also stimulates cAMP production by virtue of its stimulatory effects at tmACs and possibly soluble adenylyl cyclase (sAC) (12,13). Here we investigated potential "cross talk" among glucose metabolism, cAMP signaling, and Cdc42-Pak1 activation as it pertains to cytoskeletal remodeling and insulin secretion from human islets and rat INS-1 832/13 cells. The impact of the selective Epac activator 8-(4-chlorophenylthio)-2′-*O*-methyladenosine-3′,5′-cyclic monophosphate, acetoxymethyl ester (8-pCPT-2′-*O*-Me-cAMP-AM) (14) was compared with that of a novel cAMP antagonist (8-bromoadenosine-3′,5′-cyclic monophosphorothioate, Rp-isomer, 4-acetoxybenzyl ester [Rp-8-Br-cAMPS-pAB]) (15), while also evaluating the action of a specific inhibitor of sAC (6-chloro-N4-cyclopropyl-N4-((thiophen-3-yl)methyl) pyrimidine-2,4-diamine; also known as LRE1) (16). Remarkably, 8-pCPT-2′-*O*-Me-cAMP-AM activated Cdc42 and Pak1 in nondiabetic human islets and INS-1 832/13 cells, while also restoring Cdc42-Pak1 activation and GSIS from T2D human islets. Thus, cAMP and Epac are key determinants of proper β-cell function in the context of T2D.

RESEARCH DESIGN AND METHODS

Materials

The G-LISA Cdc42 Activation Assay Biochem Kit (catalog #BK127) and the Cdc42 Pull-Down Activation Assay Biochem Kit (catalog #BK034) were purchased from Cytoskeleton, Inc. (Denver, CO). The rabbit polyclonal antibody #2601 for phospho-Pak1-Thr^{423}/Pak2-Thr^{402} and the rabbit polyclonal antibody #2602 for total Pak1 (phosphorylated and nonphosphorylated forms) were purchased from Cell Signaling Technology (Danvers, MA). The mouse monoclonal antibody AC-74 for β-actin was purchased from Sigma-Aldrich (St. Louis, MO). The mouse monoclonal antibody against Cdc42 (catalog #610928) was purchased from BD Transduction Laboratories (San Jose, CA).

Human Islet Culture

Human islets from donors without diabetes and donors with T2D were obtained from the Integrated Islet Distribution Program and from the University of Alberta Diabetes Institute Islet Core (perifusion studies involving LRE1) (Edmonton, Alberta, Canada) (Supplementary Table 1). Islets were maintained in medium composed of Connaught Medical Research Laboratories (CMRL)-1066 (500 mL; catalog #11530037; Thermo Fisher Scientific, Waltham, MA), 0.61 g of niacinamide, 500 μL of ITS Premix Universal Culture Supplement (catalog #CB-40351; Thermo Fisher Scientific), 835 μL of Zn_2SO_4 (10 mmol/L stock), 25 mL of sodium pyruvate (100 mmol/L stock), 5 mL of Glutamax (catalog #35050061; Thermo Fisher Scientific), 12.5 mL of HEPES (1 mol/L stock), 10% FBS, 5.6 mmol/L glucose, 100 IU/mL penicillin, and 0.1 g/L streptomycin.

INS-1 832/13 Cell Culture

INS-1 832/13 cells were provided by Dr. Christopher Newgard (Duke University Medical Center, Durham, NC) (17). Cells were cultured in RPMI 1640 medium containing 11.1 mmol/L glucose, 10% heat-inactivated FBS, 100 IU/mL penicillin, 0.1 g/L streptomycin, 1 mmol/L sodium pyruvate, 50 μmol/L β-mercaptoethanol, and 10 mmol/L HEPES (pH 7.4) while maintained in a 5% CO_2 incubator. Cells were passaged by trypsinization weekly (18). The passage numbers used for this study were 52–68.

Static Incubation Assay for GSIS

Insulin secretion from INS-1 832/13 cells or T2D human islets was measured under conditions of static incubation using Krebs-Ringer bicarbonate HEPES buffer (KRBH) (500 μL/well) in a 24-well format for INS-1 832/13 cells or 500 μL/Eppendorf tube for T2D human islets. The experimental protocol was identical to that described for Cdc42 and Pak1 activation assays (see below) except that the duration of exposure to test solutions containing low or high glucose was 30 min. BioTek Synergy (Winooski, VT) HTX Multi-Mode Plate Reader was used to perform insulin assays, Rat High Range Insulin ELISA kit (catalog #80-INSRTH-E01) from American Laboratory Products Co. (Salem, NH) was used for INS-1 832/13 cells, and the Human ELISA kit (catalog #10-1113-10) from Mercodia (Winston Salem, NC) was used for T2D human islets.

Perifusion Assay for GSIS

Spontaneous formation of pseudoislets was achieved by overnight culture of INS-1 832/13 cells in six-well plates coated with 1% gelatin (catalog #G-2500; Sigma-Aldrich).

Batches of pseudoislets or human islets were loaded onto filter beds placed within 275-μL chambers, and GSIS was measured using a Biorep Technologies Inc. (Miami, FL) perifusion system (catalog #PERI4-02) interfaced with an Orbitor RS Robotic Microplate Fraction Collector (Thermo Fisher Scientific). The perifusate contained the following (in mmol/L): 120 NaCl, 24 $NaHCO_3$, 4.8 KCl, 2.5 $CaCl_2$, 1.2 $MgCl_2$, 10 HEPES, 0.1% fatty acid-free BSA (pH 7.4), and the indicated concentrations of glucose. This solution was delivered to perifusion chambers through silicone tubing at 37°C at a rate of 100 μL/min. Fractions of the perifusate were collected in 96-well plates on a cooled tray. Released insulin was measured using an ELISA kit for human insulin (catalog #10-1132-01; Mercodia), and for the INS-1 832/13 pseudoislets, Mercodia Insulin ELISA kit (catalog #10-1247-10) was used. A DC Protein Assay kit (catalog #5000116; Bio-Rad Laboratories, Hercules, CA) was used to determine the total protein content for each batch of pseudoislets or human islets.

Cdc42 and Pak1 Activation Assay Conditions

INS-1 832/13 cells were equilibrated in low-glucose (1 mmol/L) and low-serum (2.5%) culture medium overnight, whereas human islets were maintained in CMRL-1066 media for 2 h, followed by a 1 h exposure to glucose-free KRBH containing the following (in mmol/L): 140 NaCl, 3.6 KCl, 0.5 KH_2PO_4, 0.5 $MgSO_4$, 2.5 $CaCl_2$, 25 $NaHCO_3$, and 10 HEPES (pH 7.4). The KRBH was oxygenated with O_2 gas, after which 0.1% w/v fatty acid–free BSA was added (catalog #A 6003; Sigma-Aldrich). For cAMP antagonism, cells were exposed to KRBH containing Rp-8-Br-cAMPS-pAB (10 μmol/L) or 4-ABn-OH (10 μmol/L) serving as a negative control. For Epac or PKA activation, the KRBH contained 8-pCPT-2′-*O*-Me-cAMP-AM (10 μmol/L), 6-Bnz-cAMP-AM (10 μmol/L), or PO_4-AM_3 (3.3 μmol/L), serving as a negative control. Since these solutions also contained 0.1% DMSO, the standard vehicle solution for all experiment was KRBH containing 0.1% DMSO. INS-1 832/13 cells and human islets were pretreated at low glucose concentration (1 mmol/L) with each test solution for 20 min, after which the experiment was conducted at 37°C for 2 min (Cdc42 activation) or 5 min (Pak1 activation) using fresh test solutions and low (1 mmol/L) or high glucose (20 mmol/L) concentrations. Cells were then lysed in 1% NP40 buffer containing concentrations of the protease inhibitors phenylmethylsulfonyl fluoride and Na_3VO_4 of 1 mmol/L each, as well as 50 mmol/L NaF.

G-LISA Assay for Cdc42 Activation

Cell lysates were added to individual wells of a 96-well plate so that active Cdc42-GTP would be immobilized by immunoaffinity to the bottom surface of each well. Washing steps removed inactive Cdc42-GDP so that Cdc42-GTP remaining in each well could be detected using an anti-Cdc42 antibody in combination with a secondary antibody conjugated to horseradish peroxidase (HRP). Oxidation of an added substrate was monitored so that the reaction product could be quantified using a BioTek Synergy HTX Multi-Mode Plate Reader.

Pak1 Activation Assay

The phosphorylation status of Pak1 was determined by SDS-PAGE in combination with Western blot analysis. For detection of active Pak1, the assay used a 1:1,000 dilution of the #2601 rabbit polyclonal antibody that is described in the MATERIALS section (detects phospho-Pak1 or Pak2 at ~68 and 58 kDa, respectively). As a control for equivalent protein loading in individual wells of the polyacrylamide gel, the content of β-actin was detected using a mouse monoclonal antibody. Goat anti-rabbit (1:3,000) or goat anti-mouse (1:10,000) HRP-conjugated secondary antibodies were used for enhanced chemiluminescence (ECL) detection using a ChemiDoc XRS+ imaging system and an ECL/Prime Kit.

Determination of Globular Actin and Filamentous Actin Content

The globular actin (G-actin) and filamentous actin (F-actin) content was quantified using a G-Actin/F-Actin In Vivo Assay Biochem Kit (catalog #BK037; Cytoskeleton, Inc.). Briefly, cells were treated with the 0.1% DMSO vehicle control, 4-Abn-OH, or Rp-8-Br-cAMPS-pAB test solutions in the absence or presence of low (1 mmol/L) or high (20 mmol/L) concentrations of glucose. Cells were then lysed in LAS2 buffer (pH 6.9) to disrupt the cell membrane, while at the same time stabilizing and maintaining the G and F forms of actin. After centrifugation of the lysate (350*g*, 23°C, 5 min), the supernatant fraction was further centrifuged at 100,000*g* to separate F-actin (pellet) from soluble G-actin (supernatant). F-actin and G-actin were resolved by 10% SDS-PAGE and transferred to Immun-Blot PVDF Membrane for Western blot analysis using a 1:5,000 dilution of a primary anti-actin rabbit polyclonal antibody (provided in the kit) in combination with an HRP-conjugated secondary antibody (1:10,000). Proteins were detected by ECL.

Statistics

The reproducibility of findings was confirmed by performing each experiment two to five times. Data in Fig. 1 were evaluated for statistical significance by Student *t* test. For all subsequent figures, ANOVA/Bonferroni post hoc tests were used. $P < 0.05$ was considered to be statistically significant.

RESULTS

Cdc42-Pak1 Activation Is Defective in T2D Human Islets

Pak1 protein levels are 80% lower in islets from individuals with T2D compared with those from individuals who do not have diabetes (6). In addition, skeletal muscle from individuals with T2D is defective in stimulus-induced Pak1 activation events (e.g., Pak1-Thr^{423} phosphorylation) (18). Consistent with these prior findings, glucose-induced Pak1 phosphorylation in islets from humans with T2D was defective (Fig. 1*A*), as evaluated by using an anti-phospho-Pak

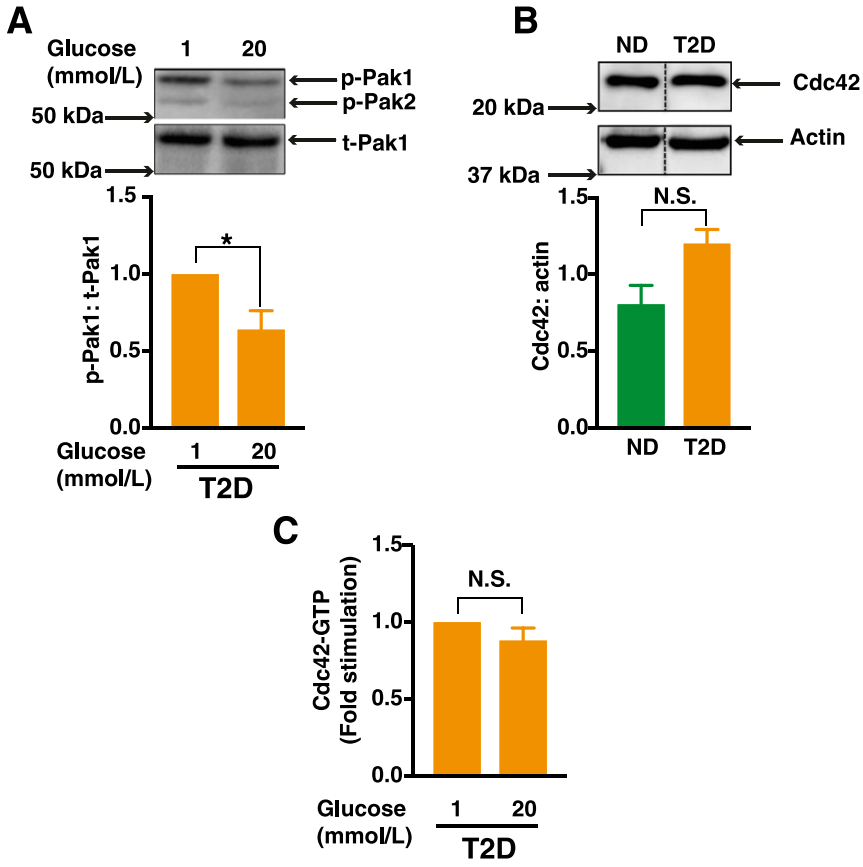

Figure 1— Defective activation of Pak1 and Cdc42 in islets from human donors with T2D. *A*: Human T2D islets were allowed to recover for 2 h in CMRL media and were then further incubated for 1 h with KRBH prior to each experiment. Islets were then incubated in the presence of either a low (1 mmol/L) or high (20 mmol/L) glucose concentration for 5 min. Pak1 activity (phosphorylation of Pak1 [p-Pak1] Thr^{423}) was normalized to total Pak1 (t-Pak1) protein content by Western blot analysis. Densitometry analysis of $n = 3$ independent experiments, shown as the mean ± SEM; $^*P < 0.05$ vs. 1 mmol/L glucose concentration. *B*: Cdc42 expression from islets from humans without diabetes (ND) ($n = 5$) or islets from humans with T2D ($n = 5$). Densitometry analysis of $n = 5$ independent experiments, shown as the mean ± SEM; black vertical dashed lines indicate the splicing of lanes from within the same gel exposure. *C*: T2D islets incubated either in the presence of low (1 mmol/L) or high (20 mmol/L) glucose for 2 min prior to their lysis. Cdc42-GTP was quantified by the G-LISA method. Data represent the mean ± SEM from $n = 3$ independent experiments. $P > 0.05$. N.S., not significant.

antibody commonly used to detect phospho-Pak1 or Pak2 at ~68 and 58 kDa, respectively, in islet β-cells (6–8). Pak1 in β-cells is activated upon the glucose-induced GTP loading of Cdc42 (5–7). Therefore, we assessed the activation of Cdc42 in islets from humans with T2D, using the high-sensitivity G-LISA method that is ideal for islets from humans with T2D, given their limited supply. This approach yielded results comparable to classic bead-based pull-down assays in studies of INS-1 832/13 cells (Supplementary Fig. 1). Cdc42 protein levels were similar in islets from humans with T2D and those without T2D (Fig. 1*B*). Although glucose stimulated Cdc42 activation was blunted in islets from humans with T2D (Fig. 1*C*), islets from humans without T2D were previously reported to show a 1.5- to 2.0-fold elevation in Cdc42 activation after exposure to glucose (7).

8-pCPT-2′-*O*-Me-cAMP-AM Activates Cdc42 and Pak1 in INS-1 832/13 Cells

We next examined a potential role for cAMP in Cdc42-Pak1 activation. It is already established that GLP-1 receptor agonists restore GSIS in patients with T2D (19,20), which is largely attributed to cAMP generation in β-cells (21). However, since the experiments reported here were performed in the absence of GLP-1, and since glucose metabolism alone also increases levels of cAMP in β-cells (22–25), we hypothesized that a nonconventional cAMP signaling mechanism that operates independently of GPCRs might also be exploited to restore insulin release in individuals with T2D. As a first test of this hypothesis, we used the selective Epac activator 8-pCPT-2′-*O*-Me-cAMP-AM (Supplementary Fig. 2), a prodrug with high membrane permeability that undergoes bioactivation catalyzed by cytosolic esterases (26). The Epac-activating properties of 8-pCPT-2′-*O*-Me-cAMP-AM were validated in INS-1 832/13 cells transduced with an Epac1-camps biosensor that reports an increased 485:535 nm fluorescence resonance energy transfer (FRET) ratio when it binds cAMP (27). 8-pCPT-2′-*O*-Me-cAMP-AM (10 μmol/L) and the positive control GLP-1 receptor agonist exendin-4 induced the

expected ΔFRET (Supplementary Fig. 3). However, PO_4-AM_3, a negative control phosphate tris(acetoxymethyl) ester that lacks the cyclic nucleotide moiety (26), was ineffective (Supplementary Fig. 3).

Having established that 8-pCPT-2′-*O*-Me-cAMP-AM is bioactivated in INS-1 832/13 cells, we evaluated its ability to activate Cdc42. Within 2 min after its addition, 8-pCPT-2′-*O*-Me-cAMP-AM (10 μmol/L) increased levels of active Cdc42-GTP. However, Cdc42 was not activated by PO_4-AM_3 or the vehicle solution (0.1% DMSO) (Fig. 2*A*). Cdc42 activation was transient, reverting to basal levels within 5 min of glucose stimulation. Of particular interest, 8-pCPT-2′-*O*-Me-cAMP-AM activated Cdc42 at low glucose concentration (1 mmol/L), with a magnitude of effect nearly identical to that measured in response to stimulatory glucose (20 mmol/L) alone. Levels of Cdc42-GTP were higher at 1 mmol/L glucose in the presence of the Epac activator, possibly due to the ability of 8-pCPT-2′-*O*-Me-cAMP-AM to activate Epac independently of a stimulatory concentration of glucose, and in turn, to cause Cdc42 activation at basal glucose (1 mmol/L). Furthermore, the combination of 20 mmol/L glucose plus 8-pCPT-2′-*O*-Me-cAMP-AM had a substantial additive effect on Cdc42 activation (Fig. 2*A*). These data suggest the following

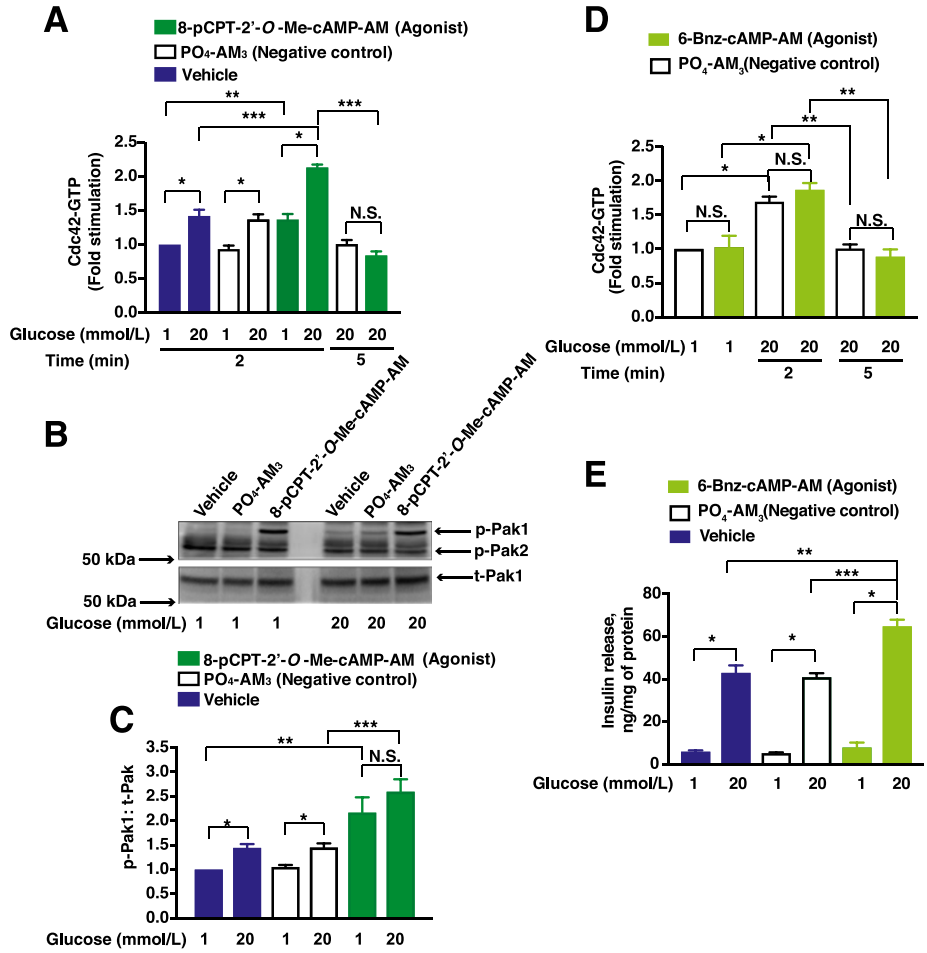

Figure 2—8-pCPT-2′-*O*-Me-cAMP-AM increases levels of Cdc42-GTP and phosphorylation of Pak1 (p-Pak1). INS-1 832/13 cells were incubated overnight in low-serum and low-glucose culture media, and further incubated for 1 h with low glucose KRBH prior to each experiment. Cells were then pretreated for 20 min with low-glucose solutions containing the vehicle, PO_4-AM_3 (3.3 μmol/L), 8-pCPT-2′-*O*-Me-cAMP-AM (10 μmol/L), or 6-Bnz-cAMP-AM (10 μmol/L). Cells were then exposed for an additional 2 or 5 min (for Cdc42 activation assay) and 5 min (for p-Pak1) to KRBH containing either low glucose (1 mmol/L) or high glucose (20 mmol/L) prior to their lysis. Cdc42-GTP was quantified by the G-LISA method. *A*: Data represent the mean ± SEM from $n = 3$ independent experiments; $^*P < 0.05$ vs. 1 mmol/L glucose within the respective treatment group; $^{**}P < 0.05$ vs. 1 mmol/L glucose treated with vehicle; $^{***}P < 0.05$, 20 mmol/L glucose treated with 8-pCPT-2′-*O*-Me-cAMP-AM vs. vehicle; $^{***}P < 0.05$, 20 mmol/L glucose treated with 8-pCPT-2′-*O*-Me-cAMP-AM at 5 min vs. at 2 min. N.S., not significant. *B*: Representative immunoblots from one of four experiments demonstrate the p-Pak1 vs. total Pak1 (t-Pak1). *C*: Densitometry analysis of $n = 4$ independent experiments, shown as the mean ± SEM; $^*P < 0.05$ vs. 1 mmol/L glucose with vehicle or PO_4-AM_3; $^{**}P < 0.05$ vs. 1 mmol/L glucose treated with vehicle; $^{***}P < 0.05$ vs. 20 mmol/L glucose with PO_4-AM_3. N.S., not significant. *D*: Data represent the mean ± SEM from $n = 3$ independent experiments; $^*P < 0.05$ vs. 1 mmol/L glucose within the respective treatment group; $^{**}P < 0.05$ vs. 20 mmol/L glucose treated with PO_4-AM_3 at 2 min. N.S., not significant. *E*: Data represent the mean ± SEM from $n = 3$ independent experiments; $^*P < 0.05$ vs. 1 mmol/L glucose within the respective treatment group; $^{**}P < 0.05$ vs. 20 mmol/L glucose treated with vehicle; $^{***}P < 0.05$ vs. 20 mmol/L glucose treated with PO_4-AM_3.

two possible mechanisms of Cdc42 activation: *1*) 8-pCPT-2′-*O*-Me-cAMP-AM and stimulatory glucose exert independent but additive effects to activate Cdc42; or *2*) the ability of 8-pCPT-2′-*O*-Me-cAMP-AM to activate Cdc42 at a basal glucose concentration (1 mmol/L) is further enhanced by a high concentration of glucose (20 mmol/L).

Next, we evaluated the influence of 8-pCPT-2′-*O*-Me-cAMP-AM on Pak1 phosphorylation. INS-1 832/13 cells in low glucose solution showed a greater than twofold increase in Thr^{423} Pak1 phosphorylation within 5 min of the addition of 8-pCPT-2′-*O*-Me-cAMP-AM (10 μmol/L) (Fig. 2*B* and *C*). However, increased Pak1 phosphorylation was not significantly increased for cells treated with PO_4-AM_3 or vehicle solution when averaging the outcomes of multiple experiments (Fig. 2*B* and *C*). Although 8-pCPT-2′-*O*-Me-cAMP-AM alone increased the levels of phosphorylated Pak1, it is important to note that at these early time points the magnitude of Cdc42 activation (Fig. 2*A*) was not exactly proportional to the magnitude of Pak1 phosphorylation (Fig. 2*B* and *C*). This is understandable since Cdc42-GTP had cycled back to inactive Cdc42-GDP within 5 min of glucose stimulation (Fig. 2*A*), whereas phosphorylated Pak1 continued to accumulate. Finally, we used the selective PKA activator prodrug 6-Bnz-cAMP-AM (N^6-benzoyladenosine-3′,5′-cyclic monophosphate, acetoxymethyl ester) (26) to investigate a potential role for PKA in Cdc42 activation. Although glucose (20 mmol/L) increased the levels of Cdc42 within 2 min after its addition, 6-Bnz-cAMP-AM failed to augment this effect despite the fact that it potentiated GSIS (Fig. 2*D* and *E*).

Rp-8-Br-cAMPS-pAB, a Potent cAMP Antagonist, Inhibits GSIS

Rp-8-Br-cAMPS-pAB (Supplementary Fig. 2) is a membrane-permeable pAB ester that undergoes bioactivation catalyzed by cytosolic esterases (15) and liberates free Rp-8-Br-cAMPS that acts as a cAMP antagonist through direct binding to PKA or Epac (15). Rp-8-Br-cAMPS-pAB is a cAMP antagonist in INS-1 832/13 cells, as demonstrated in FRET assays using cells virally transduced with an A-kinase activity reporter (AKAR3) that undergoes an increase in its 535:485 nm FRET ratio in response to PKA phosphorylation (Supplementary Figs. 4 and 5) (28,29). These assays demonstrated the ability of Rp-8-Br-cAMPS-pAB to dose-dependently block the ΔFRET measured in response to the cAMP-elevating agent forskolin (Supplementary Fig. 4).

We next performed side-by-side comparisons of GSIS in static incubation assays using INS-1 832/13 cell monolayers treated with Rp-8-Br-cAMPS-pAB (10 μmol/L) or the negative control 4-acetoxybenzyl alcohol (4-Abn-OH) (10 μmol/L). As previously reported (15), both compounds generate the side products acetic acid and 4-hydroxybenzyl alcohol when they are hydrolyzed by cytosolic esterases, yet only Rp-8-Br-cAMPS-pAB liberates free Rp-8-Br-cAMPS. It was established that Rp-8-Br-cAMPS-pAB strongly suppressed GSIS, whereas 4-Abn-OH did not (Fig. 3*A*).

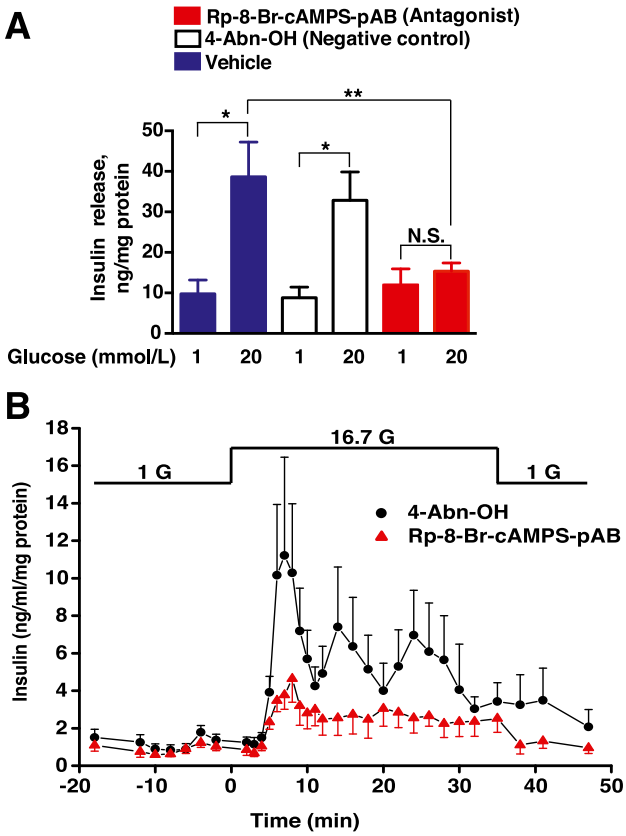

Figure 3—Rp-8-Br-cAMPS-pAB inhibits GSIS from INS-1 832/13 cells. Rp-8-Br-cAMPS-pAB (10 μmol/L) and 4-Abn-OH (10 μmol/L) were tested for their abilities to alter GSIS in 30-min static incubation assays using INS-1 832/13 cell monolayers (*A*) or in perifusion assays using pseudoislets (*B*). Rp-8-Br-cAMPS-pAB and 4-Abn-OH were each dissolved in a KRBH vehicle solution containing 0.1% DMSO and either low or high concentrations of glucose (1 G, 1 mmol/L glucose; 16.7 G, 16.7 mmol/L glucose). Data points for *A* indicate the mean ± SEM for $n = 3$ independent experiments; $^*P <$ 0.05 vs. 1 mmol/L glucose in the presence of the vehicle or 4-Abn-OH; $^{**}P < 0.05$ vs. 20 mmol/L glucose in the presence of the vehicle. Data points for *B* indicate the mean ± SEM for $n = 3$ independent experiments. Values of secreted insulin were normalized relative to the total cellular protein content. N.S., not significant.

We also performed perifusion assays to monitor the kinetics of insulin secretion from pseudoislets prepared from clusters of INS-1 832/13 cells (Supplementary Fig. 6). For pseudoislets treated with 4-Abn-OH (10 μmol/L), GSIS was measured as a transient first phase that lasted 7.5 min, followed by a sustained second phase during the continual 10- to 38-min exposure to stimulatory glucose (16.7 mmol/L) (Fig. 3*B*). Importantly, Rp-8-BrcAMPS-pAB (10 μmol/L) reduced the magnitudes of first- and second-phase GSIS under these conditions of perifusion (Fig. 3*B*). Thus, Rp-8-Br-cAMPS-pAB acted as a cAMP antagonist to suppress GSIS.

sAC Inhibition by LRE1 Fails to Block GSIS

At least two hypotheses exist to explain how glucose metabolism stimulates cAMP production in β-cells: *1*) via tmAC (22,30); or *2*) via sAC (31,32). Since sAC knockout

mice exhibit dysregulated glucose homeostasis and reduced pancreatic insulin secretion (32), we evaluated a role for sAC in GSIS using the new sAC inhibitor LRE1 (16). The capacity of LRE1 to inhibit sAC was validated in AKAR3 FRET assays that used HEK293 cells stably transfected with recombinant sAC (Supplementary Fig. 7). However, LRE1 (50 μmol/L) failed to suppress 16.7 mmol/L GSIS from perifused human islets and INS-1 832/13 pseudoislets (Fig. 4*A* and *B*). Static incubation assays using INS-1 832/13 cell monolayers further established that 5 or 10 μmol/L LRE1 failed to suppress GSIS under conditions of low (1 mmol/L) or high (20 mmol/L) glucose concentration (Fig. 4*C*).

When tested at 50 μmol/L under conditions of static incubation, LRE1 paradoxically increased both basal and stimulated insulin secretion compared with control (Fig. 4*C*). However, the stimulation index (stimulated/basal) was reduced overall (Fig. 4*C*). Since basal insulin secretion from perifused INS-1 832/13 pseudoislets or human islets (Fig. 4*A* and *B*) was unaffected by 50 μmol/L LRE1, it seems likely that the static incubation assay may favor an off-target sAC-independent effect of LRE1. For example,

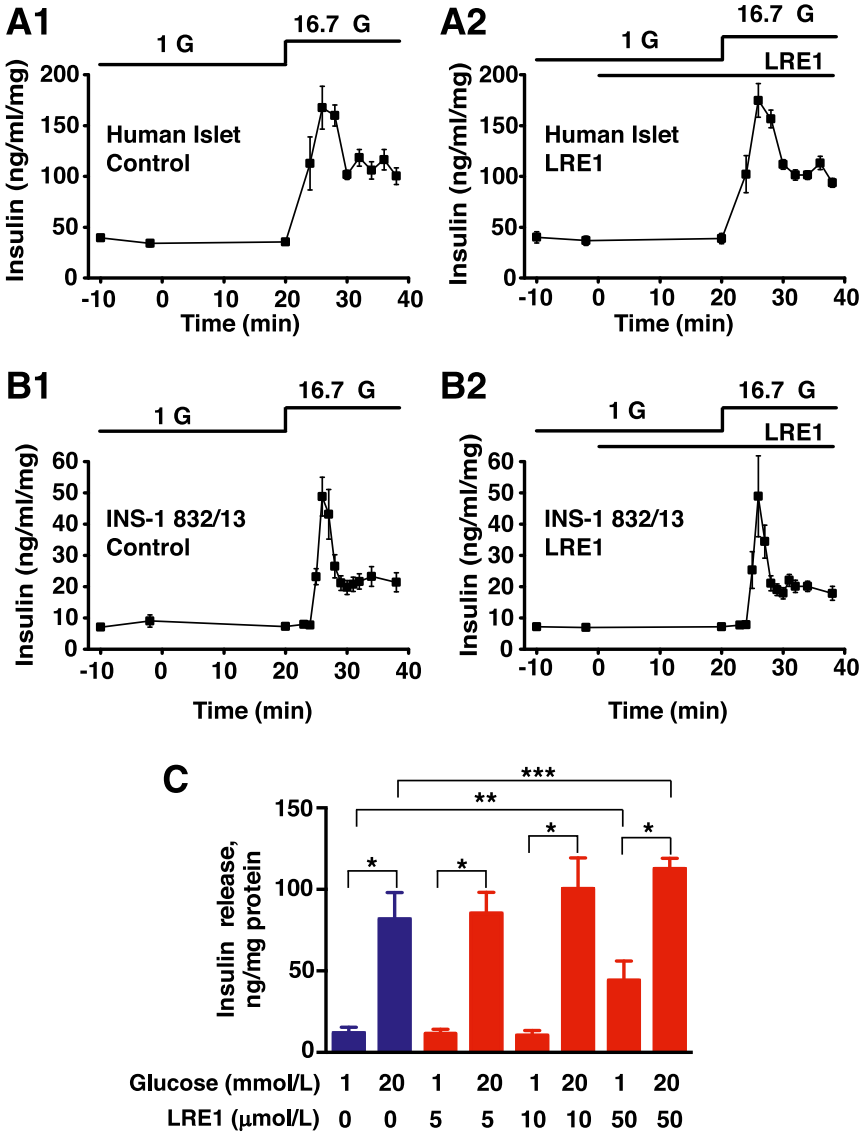

Figure 4—LRE1 fails to inhibit GSIS from human islets and INS-1 832/13 cells. LRE1 failed to inhibit basal (1 mmol/L glucose) or stimulated (20 mmol/L glucose) insulin secretion from perifused human islets (*A1* and *A2*) and perifused INS-1 832/13 pseudoislets (*B1* and *B2*). *C*: LRE1 also failed to inhibit GSIS from monolayers of INS-1 832/13 cells in static incubation assays. Values of secreted insulin in (*A*–*C*) were normalized relative to the total cellular protein content. For perifusion assays, LRE1 was tested at a concentration of 50 μmol/L (*A* and *B*) dissolved in solutions containing 1 or 16.7 mmol/L glucose (G). Data for human islets indicate the mean ± SD for $n = 2$ independent experiments (*A1* and *A2*). Data for perifused INS-1 832/13 pseudoislets indicate the mean ± SEM for $n = 3$ independent experiments (*B1* and *B2*). Data for static incubations of INS-1 832/13 cells indicate the mean ± SEM for $n = 3$ independent experiments (*C*); *$P < 0.05$ vs. 1 mmol/L glucose; **$P < 0.05$ vs. 1 mmol/L glucose in the absence of LRE1; ***$P < 0.05$ vs. 20 mmol/L glucose in the absence of LRE1.

LRE1 metabolites might accumulate intracellularly, thereby influencing insulin secretion. Collectively, these data indicate that under the experimental conditions reported here, sAC activity was not an essential factor for GSIS. However, an important caveat to this interpretation is that the exact identity of the sAC isoform expressed in β-cells has yet to be established, nor is it certain that this unknown isoform is LRE1 sensitive (see DISCUSSION).

Rp-8-Br-cAMPS-pAB Blocks Glucose-Stimulated Cdc42 Activation

We next evaluated the potential ability of Rp-8-Br-cAMPS-pAB to block glucose-stimulated Cdc42 activation in islets from humans without diabetes. It was determined that 20 mmol/L glucose stimulated a significant increase of active Cdc42-GTP within 2 min of its addition (Fig. 5*A*). In contrast, Rp-8-Br-cAMPS-pAB (10 μmol/L) blocked glucose-stimulated Cdc42 activation, whereas 4-Abn-OH (negative control) did not alter the response to glucose (Fig. 5*A*). Similar findings were obtained using INS-1 832/13 β-cells (Fig. 5*B*). These findings obtained in the G-LISA assay were independently confirmed by use of a protein-protein interaction pull-down assay to detect Cdc42-GTP by Western blot analysis using cell lysates (Supplementary Fig. 1). Thus, these findings indicate that glucose-stimulated Cdc42 activation in human islets and INS-1 832/13 cells is cAMP dependent.

Rp-8-Br-cAMPS-pAB Blocks Glucose-Stimulated Pak1 Phosphorylation

Pak1 phosphorylation was stimulated by exposure of human islets or INS-1 832/13 cells to 20 mmol/L glucose, and this action of glucose was abrogated by exposure to 10 μmol/L Rp-8-Br-cAMPS-pAB (Fig. 6*A* and *B* for human islets; Fig. 6*C* and *D* for INS-1 832/13 cells). Occasionally, we observed decreased basal levels of phospho-Pak1 for INS-1 832/13 cells treated with Rp-8-Br-cAMPS-pAB, compared with vehicle alone (Fig. 6*C* and *D*). However, this was not significant when results were averaged across multiple experiments (Fig. 6*D*). Although the anti–phospho-Pak1 antibody also detected phosphorylated Pak2, the phospho-Pak2 signal was constitutively present, and it was unaltered by Rp-8-Br-cAMPS-pAB. Note that 4-Abn-OH (10 μmol/L) failed to reproduce the inhibitory action of Rp-8-Br-cAMPS-pAB.

Rp-8-Br-cAMPS-pAB Increases F-Actin Content in INS-1 832/13 Cells

To determine whether generalized remodeling of actin is under the control of cAMP, we quantified the relative amounts of G-actin and F-actin in lysates from INS-1 832/13 cells treated with Rp-8-Br-cAMPS-pAB. As a positive control for the sensitivity of this assay, cells were treated with the F-actin–stabilizing agent phalloidin (33), which increased the F-actin content to 80% of total actin (Fig. 7). The relative amounts of G- and F-actin in whole-cell lysates were unchanged in cells treated with a low (1 mmol/L) versus high (20 mmol/L) glucose concentration (Fig. 7). This finding is expected if F-actin remodeling is localized to the cortical region of β-cells, so that such an effect is not measurable using whole-cell lysates. Notably, cells treated with Rp-8-Br-cAMPS-pAB showed significantly increased F-actin levels, regardless of the presence of either 1 or 20 mmol/L glucose (Fig. 7). These findings suggest that Rp-8-Br-cAMPS-pAB exerts an F-actin–stabilizing effect. Because the stabilization of F-actin in β-cells generally inhibits insulin release (34,35), it is understandable that Rp-8-Br-cAMPS-pAB also inhibited GSIS from INS-1 832/13 cells (Fig. 3*A* and *B*).

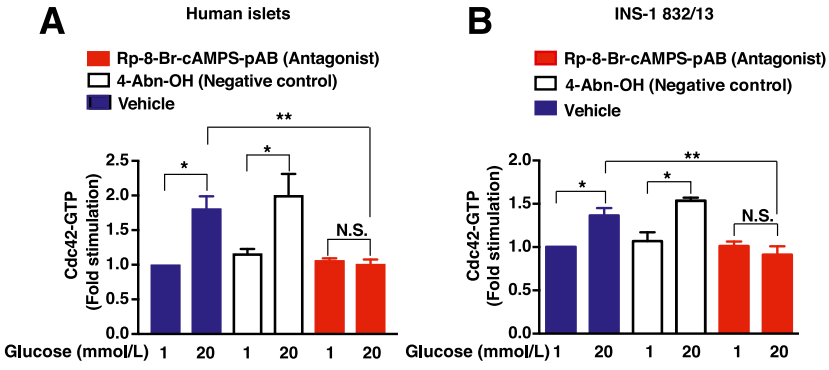

Figure 5—Rp-8-Br-cAMPS-pAB blocks Cdc42 activation in human islets and INS-1 832/13 cells. Human islets (*A*) or INS-1 832/13 cells (*B*) were pretreated for 20 min with a vehicle solution containing 1 mmol/L glucose and 0.1% DMSO dissolved in KRBH. For comparison, cells were also pretreated with 4-Abn-OH (10 μmol/L) or Rp-8-Br-cAMPS-pAB (10 μmol/L) dissolved in KRBH containing 1 mmol/L glucose and 0.1% DMSO. Cells were then treated for 2 min with KRBH containing 1 or 20 mmol/L glucose and either 0.1% DMSO, 4-Abn-OH (10 μmol/L), or Rp-8-Br-cAMPS-pAB (10 μmol/L). After lysis, Cdc42-GTP was detected by G-LISA, and a value of 1.0 was assigned to the baseline level of Cdc42-GTP detected in cells treated with the vehicle solution containing 1 mmol/L glucose alone. Data are the mean ± SEM fold-stimulation relative to baseline for $n = 3$ independent experiments in replicates; *$P < 0.05$ vs. 1 mmol/L glucose with vehicle or 4-Abn-OH; **$P < 0.05$ vs. 20 mmol/L glucose with vehicle. N.S., not significant.

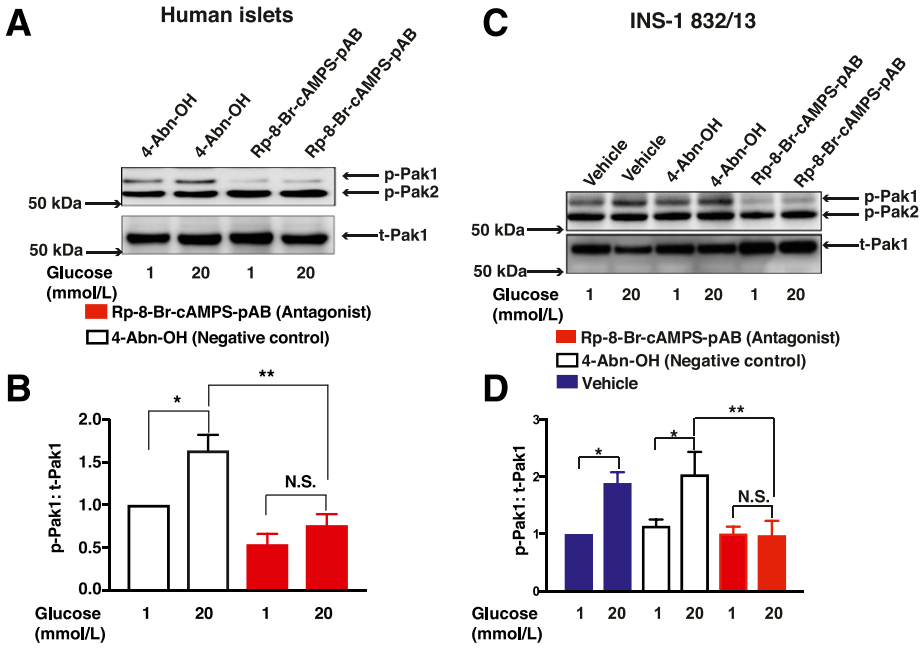

Figure 6—Rp-8-Br-cAMPS-pAB blocks Pak1 activation in human islets and INS-1 832/13 cells. Human islets (*A* and *B*) or INS-1 832/13 cells (*C* and *D*) were pretreated for 20 min with a vehicle solution composed of KRBH containing 1 mmol/L glucose and 0.1% DMSO. For comparison, cells were also pretreated with 4-Abn-OH (10 μmol/L) or Rp-8-Br-cAMPS-pAB (10 μmol/L) dissolved in KRBH containing 1 mmol/L glucose and 0.1% DMSO. Cells were then treated for 5 min with KRBH containing 1 or 20 mmol/L glucose and 0.1% DMSO, 4-Abn-OH (10 μmol/L), or Rp-8-Br-cAMPS-pAB (10 μmol/L). *A* and *C*: Immunoblots are representative of three or five identical independent experiments using human islets or INS-1 832/13 cells, respectively, showing the stimulation of Pak1 phosphorylation (p-Pak1) vs. total Pak1 (t-Pak1) present in the cell lysates. *B* and *D*: Densitometry analysis of $n = 3$ for human islets and $n = 5$ independent experiments for INS-1 832/13 cells, shown as the mean ± SEM. *$P < 0.05$ vs. 1 mmol/L glucose with vehicle or 4-Abn-OH; **$P < 0.05$ vs. 20 mmol/L glucose with 4-Abn-OH. N.S., not significant.

Cool-1/βPix Knockdown Studies for GSIS and Cdc42 Activation

It was reported that Cool-1/βPix is a GEF that mediates glucose-stimulated Cdc42 activation in MIN6 β-cells (9). Thus, Cool-1/βPix might link cAMP production and Epac2 activation to downstream activation of Cdc42. To address this issue, we used siRNA knockdown (KD) technology to deplete endogenous Cool-1/βPix in INS-1 832/13 cells treated with glucose or 8-pCPT-2′-*O*-Me-cAMP-AM (Supplementary Fig. 8). These studies demonstrated reduced glucose-stimulated Cdc42 activation accompanied by reduced GSIS in cells depleted of Cool-1/βPix. However, Cdc42 activation by 8-pCPT-2′-*O*-Me-cAMP-AM was not significantly reduced after the KD of Cool-1/βPix, although an inhibitory trend was noted. Potentiation of GSIS by 8-pCPT-2′-*O*-Me-cAMP-AM was also unaffected by a KD of Cool-1/βPix. One interpretation of these findings is that Cool-1/βPix does not mediate the action of cAMP and Epac to activate Cdc42 and to potentiate GSIS. However, it should be noted that Cool-1/βPix protein levels were depleted by ~50% in these assays, and for this reason it remains possible that residual expression of Cool-1/βPix mediates the pharmacological actions of 8-pCPT-2′-*O*-Me-cAMP-AM reported here. Clearly, a rationale exists to repeat such studies using islets of Cool-1/βPix knockout mice in which residual expression of Cool-1/βPix is not a complicating factor.

8-pCPT-2′-*O*-Me-cAMP-AM Restores GSIS and Cdc42-Pak1 Activation in Islets From Humans With T2D

Findings summarized above led us to hypothesize that an Epac activator would restore GSIS from T2D human islets by virtue of its ability to promote Cdc42-Pak1 activation. This was in fact the case since treatment with 8-pCPT-2′-*O*-Me-cAMP-AM restored 20 mmol/L GSIS leading to an approximately twofold increase of insulin secretion (Fig. 8*A*). Basal insulin secretion at 1 mmol/L glucose was not significantly altered relative to the PO_4-AM_3 negative control (Fig. 8*A*). Remarkably, in T2D islets, 8-pCPT-2′-*O*-Me-cAMP-AM also restored glucose-stimulated Cdc42 activation (Fig. 8*B*) and Pak1 phosphorylation (Fig. 8*C* and *D*).

DISCUSSION

The primary goal of this study was to determine whether cAMP participates in signaling events that link β-cell glucose metabolism to Cdc42-Pak1 activation, F-actin remodeling, and insulin secretion. We also sought to determine whether some of these key signaling steps could be restored in T2D human islets after exposure to an Epac-selective cAMP analog that we hypothesized would emulate the restorative action of GLP-1 in islet β-cells. Initially, we found that the cAMP antagonist Rp-8-Br-cAMPS-pAB suppressed glucose-stimulated Cdc42-Pak1 activation, while stabilizing F-actin and inhibiting GSIS in the absence

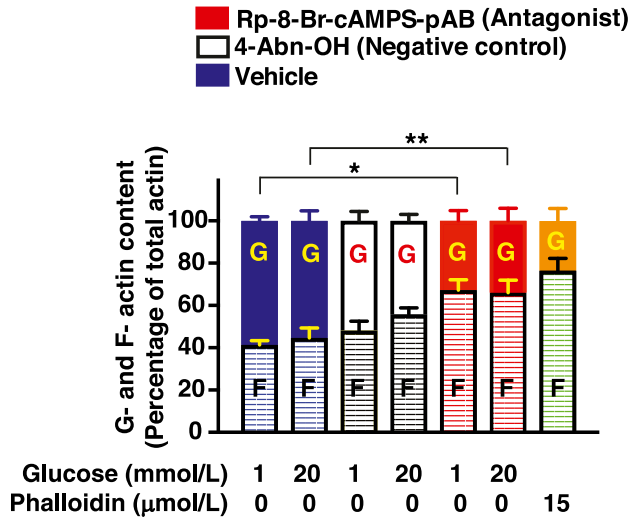

Figure 7—Rp-8-Br-cAMPS-pAB alters the G-actin (G)/F-actin (F) ratio. INS-1 832/13 cells were incubated overnight in low-serum and low-glucose culture media and were further incubated for 1 h with low-glucose KRBH prior to each experiment. Cells were then pretreated for 20 min with low-glucose KRBH containing the vehicle, 4-Abn-OH (10 μmol/L), or Rp-8-Br-cAMPS-pAB (10 μmol/L). Next, cells were exposed for 5 min to KRBH containing low glucose (1 mmol/L) or high glucose (20 mmol/L) prior to lysis in a buffer that solubilizes G-actin but not F-actin. Centrifugation was used to pellet F-actin while leaving G-actin in the supernatant. Proteins were subjected to 10% SDS-PAGE and Western blot analysis to detect G- and F-actin. Densitometry analysis of three independent experiments is shown as the mean ± SEM. The *y*-axis scaling indicates the percentage of total actin; $^{*}P < 0.05$ vs. 1 mmol/L glucose in the presence of vehicle; $^{**}P < 0.05$ vs. 20 mmol/L glucose in the presence of vehicle.

of cAMP-elevating agents such as GLP-1. Such findings illuminate a previously unappreciated role for cAMP as a permissive factor, or possibly as a direct metabolic coupling factor, in support of glucose-stimulated Cdc42-Pak1 activation, F-actin remodeling, and GSIS. These actions of cAMP complement its previously established ability to participate in the control of β-cell K_{ATP} channels, cytosolic Ca^{2+} dynamics, and insulin exocytosis (21). Currently, there is great interest to determine the sources of this cAMP and to identify which processes are under the control of PKA and/or Epac.

PKA was previously suggested to play a dominant role in the control of GSIS on the basis of studies using mice that harbored an activating mutation in a PKA catalytic subunit isoform (36) or had genetic deletion of a PKA regulatory subunit isoform (37). However, we found that the Epac activator 8-pCPT-2′-*O*-Me-cAMP-AM promoted Cdc42-Pak1 activation, whereas the PKA activator 6-Bnz-cAMP-AM was less effective. Since 8-pCPT-2′-*O*-Me-cAMP-AM potentiates GSIS (38,39), Epac may mediate an action of cAMP to enable glucose-stimulated Cdc42-Pak1 activation. Intriguingly, Epac2 knockout mice fed a high-fat diet do not exhibit the compensatory upregulation of GSIS that is characteristic of wild-type mice fed the same high-fat diet (40,41). These in vivo findings are consistent with reports that Epac2 is expressed in β-cells (11).

We found that Rp-8-Br-cAMPS-pAB reduced levels of Cdc42-GTP and p-Pak1 under conditions of stimulatory (20 mmol/L) but not basal (1 mmol/L) glucose. Rp-8-Br-cAMPS-pAB also increased whole-cell F-actin content in INS-1 832/13 cells, as expected if it exerted a stabilizing effect to counteract glucose-stimulated and cAMP-dependent F-actin depolymerization. This stabilizing effect was present in cells exposed to stimulatory (20 mmol/L) or basal (1 mmol/L) glucose. Thus, unlike results obtained with the Cdc42-Pak1 assays, the F-actin–stabilizing effect of Rp-8-Br-cAMPS-pAB did not necessarily depend on metabolic signaling induced by stimulatory glucose. One possible explanation is that 1 mmol/L glucose supports low-level cAMP production, and therefore basal PKA activity. If so, Rp-8-Br-cAMPS-pAB might block basal F-actin remodeling that is supported by basal PKA activity and that is not contingent on Cdc42-Pak1 activation occurring at stimulatory concentrations of glucose, which might instead promote additional F-actin remodeling that is Epac2 dependent. Measurement of this basal PKA activity will require the targeting of biosensors to select subcellular compartments rather than the use of a globally expressed AKAR3.

In addition to Cdc42-Pak1, there are other key players in regulated exocytosis of insulin. These include the cytoskeletal regulatory proteins LIMK1, cofilin, N-WASP, and Arp2/3 that participate in F-actin remodeling (42) and that might be cAMP regulated. Importantly, the inhibitory actions of Rp-8-Br-cAMPS-AM reported here in assays of GSIS were not simply explained by a disruption of cytosolic Ca^{2+} dynamics that normally trigger insulin exocytosis. In fact, we found that this cAMP antagonist increased intracellular Ca^{2+} concentrations in INS-1 832/13 cells (Supplementary Fig. 9). This was an unanticipated finding because voltage-dependent Ca^{2+} channels require permissive PKA activity in order to allow glucose-stimulated Ca^{2+} influx. However, PKA activity also regulates other types of ion channels that control the membrane potential. For example, chronic inhibition of PKA may lead to K_{ATP} channel closure (24).

Taken as a whole, the results of our studies using Rp-8-Br-cAMPS-pAB indicate that the activation of Cdc42-Pak1 by stimulatory glucose requires cAMP and Epac2 signaling that is not present at basal glucose concentrations. In this regard, Epac2 might have a lower affinity for cAMP in comparison with PKA (26). Thus, Epac2-mediated Cdc42 and/or Pak1 activation may depend on increased cAMP production at stimulatory glucose levels. This glucose dependence of Epac2 action is circumvented by pharmacological activation of Epac2 using 8-pCPT-2′-*O*-Me-cAMP-AM. Thus, 8-pCPT-2′-*O*-Me-cAMP-AM activated Cdc42-Pak1 in the presence of both 1 and 20 mmol/L glucose concentrations.

Although cAMP production stimulated by glucose is inhibited when tmAC activity is reduced (22–24), speculation still exists that sAC also mediates glucose-stimulated cAMP

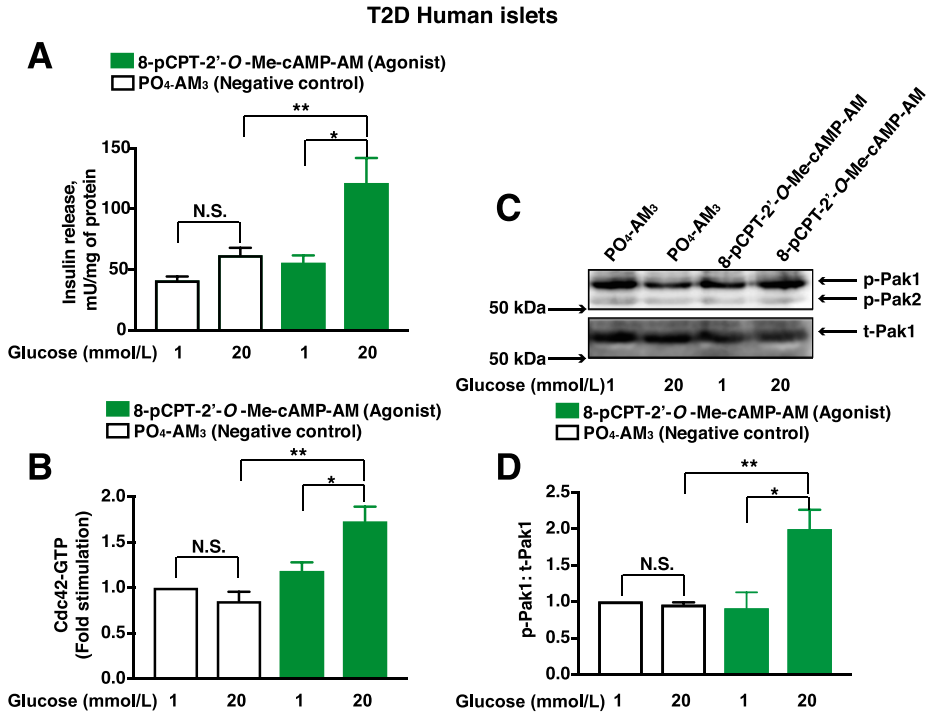

Figure 8—Restoration of Cdc42-Pak1 activation and GSIS in human T2D islets by Epac activator 8-pCPT-2′-*O*-Me-cAMP-AM. *A*: T2D islets were pretreated for 20 min with low-glucose solutions containing PO_4-AM_3 (3.3 μmol/L) or 8-pCPT-2′-*O*-Me-cAMP-AM (10 μmol/L). Islets were then exposed for 30 min to KRBH containing either a low-glucose (1 mmol/L) or high-glucose (20 mmol/L) concentration, and the supernatants were collected to measure insulin released into the media. Data represent the mean ± SEM from three independent experiments; *$P < 0.05$ vs. 1 mmol/L glucose treated with 8-pCPT-2′-*O*-Me-cAMP-AM and **$P < 0.05$ vs. 20 mmol/L glucose treated with PO_4-AM_3. *B* and *C*: T2D islets were pretreated for 20 min with low-glucose solutions containing PO_4-AM_3 (3.3 μmol/L) or 8-pCPT-2′-*O*-Me-cAMP-AM (10 μmol/L). Islets were then exposed for 2 min (*B*, Cdc42 activation) or 5 min (*C*, Pak1 activation) to KRBH containing either a low-glucose (1 mmol/L) or high-glucose (20 mmol/L) concentration prior to their lysis. Cdc42-GTP was quantified by the G-LISA method. Data represent the mean ± SEM from three independent experiments: *$P < 0.05$ vs. 1 mmol/L glucose treated with 8-pCPT-2′-*O*-Me-cAMP-AM and **$P < 0.05$ vs. 20 mmol/L glucose treated with PO_4-AM_3. *C*: Representative immunoblots from one of three experiments demonstrate the phosphorylation of Pak1 (p-Pak1) (*C*) vs. total Pak1 (t-Pak1) (*D*). Densitometry analysis of $n = 3$ independent experiments, shown as the mean ± SEM; *$P < 0.05$ vs. 1 mmol/L glucose with 8-pCPT-2′-*O*-Me-cAMP-AM and **$P < 0.05$ vs. 20 mmol/L glucose treated with PO_4-AM_3. N.S., not significant.

production in β-cells (13). Because sAC is stimulated by bicarbonate ion (HCO_3^-) (32), the coupling of glucose metabolism to sAC activation could occur if β-cell mitochondrial metabolism generates CO_2 that is converted to HCO_3^- by carbonic anhydrase (13). Furthermore, sAC is stimulated by Ca^{2+}, an ionic coupling factor that might link glucose metabolism to cAMP production in β-cells (13). For these reasons, it is surprising that LRE1, a new and specific sAC inhibitor (16), failed to inhibit GSIS from INS-1 832/13 cells and human islets. Thus, prior studies documenting defective GSIS in islets from global sAC knockout mice (32) were not corroborated in the current study by any action of LRE1 to inhibit GSIS from INS-1 832/13 cells or human islets. However, multiple isoforms of sAC exist as a consequence of alternative mRNA splicing (43), and the exact isoform of sAC expressed in β-cells has not yet been identified. Clearly, there is a need to establish the molecular identity of the β-cell sAC, and to determine to what extent its activity is inhibited by LRE1.

Finally, perhaps the most striking aspect of the findings presented here is the capacity of 8-pCPT-2′-*O*-Me-cAMP-AM to restore GSIS in islets from humans with T2D. Such findings hint at a potential defect of cAMP production and/or Epac2 activation as a contributing factor to insulin insufficiency in T2D. In this scenario, underactive cAMP/Epac2 signaling would predispose to defective GSIS, whereas a selective Epac activator would compensate for this defect by upregulating Epac2 activity. This hypothesis is consistent with the established role that Epac2 plays in multiple aspects of β-cell stimulus-secretion coupling (44,45). What remains to be demonstrated is whether GLP-1 receptor agonists used for the treatment of T2D exert their beneficial insulin secretagogue actions through the cAMP/Epac signaling pathways described here.

Conclusions

In summary, our findings provide new insight into processes of Cdc42-Pak1 activation and F-actin remodeling whereby secretory granules gain access to the plasma membrane for "docking" and "priming" events prior to exocytosis. This F-actin remodeling may also participate in cAMP-regulated "newcomer" exocytosis in which secretory

granules translocate to the plasma membrane for immediate exocytosis without pausing in a docked state (46). It is noteworthy that Epac2 mediates GLP-1 activity to restore glucose-stimulated F-actin remodeling under conditions of β-cell glucotoxicity (47). Similarly, GLP-1 signals through PKA to disassemble cytoskeletal stress fibers, promote actin depolymerization, and restore GSIS under conditions of glucotoxicity (48). These studies are complemented by our new finding that the Epac activator 8-pCPT-2′-*O*-Me-cAMP-AM restores Cdc42 activation and Pak1 phosphorylation in islets from humans with T2D. Thus, substantial opportunity exists for future studies to define which cAMP-binding proteins, cytoskeletal remodeling processes, and mechanisms of secretory granule translocation participate alone, or in combination, to stimulate insulin secretion.

Acknowledgments. The authors thank the United Network for Organ Sharing for providing donated pancreases used for isolating human islets. The authors also thank the Integrated Islet Distribution Center and Southern California Islet Cell Resource Center at City of Hope for preparing and providing the majority of the isolated islets used for this study.

Funding. This work was supported by National Institute of Diabetes and Digestive and Kidney Diseases grants to G.G.H. (R01-DK-069575) and D.C.T. (R01-DK-067912, R01-DK-102233).

Duality of Interest. F.S. is employed at BIOLOG Life Science Institute, which is selling 8-pCPT-2′-*O*-Me-cAMP-AM as a research tool. No other potential conflicts of interest relevant to this article were reported.

Author Contributions. R.V. performed static incubation assays of GSIS in addition to the G-LISA and immunoblot assays of Cdc42 activation, Pak1 activation, and actin content; was responsible for the experimental plan, literature search, and manuscript writing and editing; and read and approved the final version of the manuscript. O.G.C. performed AKAR3 and Epac1-camps FRET assays and read and approved the final version of the manuscript. C.A.L. performed pseudoislet perifusion assays of GSIS and read and approved the final version of the manuscript. F.S. synthesized and provided cAMP analogs for use in these studies and read and approved the final version of the manuscript. G.G.H. and D.C.T. were responsible for the experimental plan, literature search, and manuscript writing and editing; conceived of the project; and read and approved the final version of the manuscript. R.V. is the guarantor of this work and, as such, had full access to all the data in the study and takes responsibility for the integrity of the data and the accuracy of the data analysis.

Prior Presentation. Parts of this study were presented in abstract form at the 77th Scientific Sessions of the American Diabetes Association, San Diego, CA, 9–13 June 2017.

References

1. Prentki M, Nolan CJ. Islet beta cell failure in type 2 diabetes. J Clin Invest 2006;116:1802–1812
2. Prentki M, Matschinsky FM, Madiraju SR. Metabolic signaling in fuel-induced insulin secretion. Cell Metab 2013;18:162–185
3. Seino S, Shibasaki T, Minami K. Dynamics of insulin secretion and the clinical implications for obesity and diabetes. J Clin Invest 2011;121:2118–2125
4. Rorsman P, Braun M. Regulation of insulin secretion in human pancreatic islets. Annu Rev Physiol 2013;75:155–179
5. Wang Z, Oh E, Thurmond DC. Glucose-stimulated Cdc42 signaling is essential for the second phase of insulin secretion. J Biol Chem 2007;282:9536–9546
6. Wang Z, Oh E, Clapp DW, Chernoff J, Thurmond DC. Inhibition or ablation of p21-activated kinase (PAK1) disrupts glucose homeostatic mechanisms in vivo. J Biol Chem 2011;286:41359–41367
7. Kalwat MA, Yoder SM, Wang Z, Thurmond DCA. A p21-activated kinase (PAK1) signaling cascade coordinately regulates F-actin remodeling and insulin granule exocytosis in pancreatic β cells. Biochem Pharmacol 2013;85:808–816
8. Orci L, Gabbay KH, Malaisse WJ. Pancreatic beta-cell web: its possible role in insulin secretion. Science 1972;175:1128–1130
9. Kepner EM, Yoder SM, Oh E, et al. Cool-1/βPIX functions as a guanine nucleotide exchange factor in the cycling of Cdc42 to regulate insulin secretion. Am J Physiol Endocrinol Metab 2011;301:E1072–E1080
10. Hussain MA, Stratakis C, Kirschner L. Prkar1a in the regulation of insulin secretion. Horm Metab Res 2012;44:759–765
11. Leech CA, Chepurny OG, Holz GG. Epac2-dependent rap1 activation and the control of islet insulin secretion by glucagon-like peptide-1. Vitam Horm 2010;84:279–302
12. Tengholm A. Cyclic AMP dynamics in the pancreatic β-cell. Ups J Med Sci 2012;117:355–369
13. Holz GG, Leech CA, Chepurny OG. New insights concerning the molecular basis for defective glucoregulation in soluble adenylyl cyclase knockout mice. Biochim Biophys Acta 2014;1842:2593–2600
14. Chepurny OG, Leech CA, Kelley GG, et al. Enhanced Rap1 activation and insulin secretagogue properties of an acetoxymethyl ester of an Epac-selective cyclic AMP analog in rat INS-1 cells: studies with 8-pCPT-2′-*O*-Me-cAMP-AM. J Biol Chem 2009;284:10728–10736
15. Schwede F, Chepurny OG, Kaufholz M, et al. Rp-cAMPS prodrugs reveal the cAMP dependence of first-phase glucose-stimulated insulin secretion. Mol Endocrinol 2015;29:988–1005
16. Ramos-Espiritu L, Kleinboelting S, Navarrete FA, et al. Discovery of LRE1 as a specific and allosteric inhibitor of soluble adenylyl cyclase. Nat Chem Biol 2016;12:838–844
17. Hohmeier HE, Mulder H, Chen G, Henkel-Rieger R, Prentki M, Newgard CB. Isolation of INS-1-derived cell lines with robust ATP-sensitive K^+ channel-dependent and -independent glucose-stimulated insulin secretion. Diabetes 2000;49:424–430
18. Sylow L, Jensen TE, Kleinert M, et al. Rac1 signaling is required for insulin-stimulated glucose uptake and is dysregulated in insulin-resistant murine and human skeletal muscle. Diabetes 2013;62:1865–1875
19. Zander M, Madsbad S, Madsen JL, Holst JJ. Effect of 6-week course of glucagon-like peptide 1 on glycaemic control, insulin sensitivity, and beta-cell function in type 2 diabetes: a parallel-group study. Lancet 2002;359:824–830
20. Fehse F, Trautmann M, Holst JJ, et al. Exenatide augments first- and second-phase insulin secretion in response to intravenous glucose in subjects with type 2 diabetes. J Clin Endocrinol Metab 2005;90:5991–5997
21. Holz GG, Chepurny OG, Leech CA, Song WJ, Hussain MA. Molecular basis of cAMP signaling in pancreatic beta-cells. In *The Islets of Langerhans*. 2nd ed. Islam MS, Ed. Dordrecht, the Netherlands, Springer Netherlands, 2015, p. 565–603
22. Landa LR Jr., Harbeck M, Kaihara K, et al. Interplay of Ca^{2+} and cAMP signaling in the insulin-secreting MIN6 beta-cell line. J Biol Chem 2005;280:31294–31302
23. Dyachok O, Idevall-Hagren O, Sågetorp J, et al. Glucose-induced cyclic AMP oscillations regulate pulsatile insulin secretion. Cell Metab 2008;8:26–37
24. Idevall-Hagren O, Barg S, Gylfe E, Tengholm A. cAMP mediators of pulsatile insulin secretion from glucose-stimulated single beta-cells. J Biol Chem 2010;285:23007–23018
25. Hodson DJ, Mitchell RK, Marselli L, et al. ADCY5 couples glucose to insulin secretion in human islets. Diabetes 2014;63:3009–3021
26. Holz GG, Chepurny OG, Schwede F. Epac-selective cAMP analogs: new tools with which to evaluate the signal transduction properties of cAMP-regulated guanine nucleotide exchange factors. Cell Signal 2008;20:10–20
27. Nikolaev VO, Bünemann M, Hein L, Hannawacker A, Lohse MJ. Novel single chain cAMP sensors for receptor-induced signal propagation. J Biol Chem 2004;279:37215–37218
28. Allen MD, Zhang J. Subcellular dynamics of protein kinase A activity visualized by FRET-based reporters. Biochem Biophys Res Commun 2006;348:716–721

29. Holz GG, Leech CA, Roe MW, et al. High-throughput FRET assays for fast time-dependent detection of cyclic AMP in pancreatic beta cells. In *Cyclic Nucleotide Signaling*. Xiaodong C, Ed. Boca Raton, FL, CRC Press, 2015, p. 35–60

30. Tian G, Sandler S, Gylfe E, Tengholm A. Glucose- and hormone-induced cAMP oscillations in α- and β-cells within intact pancreatic islets. Diabetes 2011; 60:1535–1543

31. Ramos LS, Zippin JH, Kamenetsky M, Buck J, Levin LR. Glucose and GLP-1 stimulate cAMP production via distinct adenylyl cyclases in INS-1E insulinoma cells. J Gen Physiol 2008;132:329–338

32. Zippin JH, Chen Y, Straub SG, et al. CO_2/HCO_3(-)- and calcium-regulated soluble adenylyl cyclase as a physiological ATP sensor. J Biol Chem 2013;288: 33283–33291

33. Wehland J, Osborn M, Weber K. Phalloidin-induced actin polymerization in the cytoplasm of cultured cells interferes with cell locomotion and growth. Proc Natl Acad Sci U S A 1977;74:5613–5617

34. Li G, Rungger-Brändle E, Just I, Jonas JC, Aktories K, Wollheim CB. Effect of disruption of actin filaments by Clostridium botulinum C2 toxin on insulin secretion in HIT-T15 cells and pancreatic islets. Mol Biol Cell 1994;5:1199–1213

35. Jewell JL, Luo W, Oh E, Wang Z, Thurmond DC. Filamentous actin regulates insulin exocytosis through direct interaction with Syntaxin 4. J Biol Chem 2008; 283:10716–10726

36. Kaihara KA, Dickson LM, Jacobson DA, et al. β-Cell-specific protein kinase A activation enhances the efficiency of glucose control by increasing acute-phase insulin secretion. Diabetes 2013;62:1527–1536

37. Song WJ, Seshadri M, Ashraf U, et al. Snapin mediates incretin action and augments glucose-dependent insulin secretion. Cell Metab 2011;13: 308–319

38. Kelley GG, Chepurny OG, Schwede F, et al. Glucose-dependent potentiation of mouse islet insulin secretion by Epac activator 8-pCPT-2′-*O*-Me-cAMP-AM. Islets 2009;1:260–265

39. Chepurny OG, Kelley GG, Dzhura I, et al. PKA-dependent potentiation of glucose-stimulated insulin secretion by Epac activator 8-pCPT-2′-*O*-Me-cAMP-AM in human islets of Langerhans. Am J Physiol Endocrinol Metab 2010;298: E622–E633

40. Song WJ, Mondal P, Li Y, Lee SE, Hussain MA. Pancreatic β-cell response to increased metabolic demand and to pharmacologic secretagogues requires EPAC2A. Diabetes 2013;62:2796–2807

41. Holz GG, Chepurny OG, Leech CA. Epac2A makes a new impact in β-cell biology. Diabetes 2013;62:2665–2666

42. Uenishi E, Shibasaki T, Takahashi H, et al. Actin dynamics regulated by the balance of neuronal Wiskott-Aldrich syndrome protein (N-WASP) and cofilin activities determines the biphasic response of glucose-induced insulin secretion. J Biol Chem 2013;288:25851–25864

43. Jaiswal BS, Conti M. Identification and functional analysis of splice variants of the germ cell soluble adenylyl cyclase. J Biol Chem 2001;276: 31698–31708

44. Holz GG. Epac: a new cAMP-binding protein in support of glucagon-like peptide-1 receptor-mediated signal transduction in the pancreatic beta-cell. Diabetes 2004;53:5–13

45. Holz GG, Kang G, Harbeck M, Roe MW, Chepurny OG. Cell physiology of cAMP sensor Epac. J Physiol 2006;577:5–15

46. Shibasaki T, Takahashi H, Miki T, et al. Essential role of Epac2/Rap1 signaling in regulation of insulin granule dynamics by cAMP. Proc Natl Acad Sci U S A 2007; 104:19333–19338

47. Quinault A, Gausseres B, Bailbe D, et al. Disrupted dynamics of F-actin and insulin granule fusion in INS-1 832/13 beta-cells exposed to glucotoxicity: partial restoration by glucagon-like peptide 1. Biochim Biophys Acta 2016;1862:1401–1411

48. Kong X, Yan D, Sun J, et al. Glucagon-like peptide 1 stimulates insulin secretion via inhibiting RhoA/ROCK signaling and disassembling glucotoxicity-induced stress fibers. Endocrinology 2014;155:4676–4685